

Northern Hemisphere Five-Year Average (2000-2004) Spectral Snow Albedos: Statistics Computed from Terra MODIS Land Products

ERIC G. MOODY,^{*} MICHAEL D. KING,⁺ CRYSTAL B. SCHAAF,[#]
DOROTHY K. HALL,[@] AND STEVEN PLATNICK⁺

^{}L-3 Communications Government Services, Inc., Vienna, Virginia*

*⁺Earth-Sun Exploration Division, NASA Goddard Space Flight Center, Greenbelt,
Maryland*

*[#]Center for Remote Sensing, Department of Geography, Boston University, Boston,
Massachusetts*

*[@]Hydrospheric and Biospheric Sciences Laboratory, NASA Goddard Space Flight Cen-
ter, Greenbelt, Maryland*

Journal of Climate

(Manuscript submitted January 2006)

Corresponding author address: Eric G. Moody, L-3 Communications Govern-
ment Services, Inc., Vienna, VA 22180 USA.

E-mail: moody@climate.gsfc.nasa.gov.

ABSTRACT

In this paper, we present a five-year (2000-2004) mean and standard deviation of Northern Hemisphere spectral white-sky snow albedo for the 16 International Geosphere-Biosphere Program (IGBP) ecosystem classes. These statistics are obtained using calibrated, high quality Moderate Resolution Imaging Spectroradiometer (MODIS) land surface albedo (MOD43B3) data flagged as snow in the associated Quality Assurance (QA) fields. Near Real-Time Ice and Snow Extent (NISE) data are used as an additional discriminator of snow extent. Statistics are provided for the first seven MODIS bands, ranging from 0.47 to 2.1 μm , and for three broadbands, 0.3-0.7, 0.3-5.0 and 0.7-5.0 μm .

The statistics demonstrate that each ecosystem classification has a unique spectral snow albedo signature. This indicates that both the winter canopy and underlying surface radiative properties impact the reflectivity of the snow overlying these surfaces. For example, although the white-sky albedo of permanent snow surfaces such as Greenland and Antarctica is shown to be as high as 0.950 at 0.47 μm , snow-covered evergreen needleleaf forests may have a white-sky albedo as low as 0.356 at 0.47 μm . All 16 ecosystems considered in this study exhibit substantial reductions in albedo in the near-infrared and all surfaces have an albedo of about 0.06 at 2.13 μm . These statistics can be used to force land surface models in a stand-alone mode, prescribe albedo values in atmospheric General Circulation Models (GCMs), or can be incorporated into research and operational projects. They are intended to provide researchers with representative spectral snow albedo values that are derived from validated satellite data.

1. Introduction

The spectral albedo of snow plays an important role in various Earth system research projects because it quantifies the amount of incident solar radiation absorbed by the Earth's surface. However, the albedo of snow can vary dramatically and thereby affect radiative transfer calculations. There are several important factors that influence the albedo of a snow-covered surface, namely the snow state (e.g., dry *vs.* wet snow), morphology, age, snow depth, contamination of the snow by absorptive materials such as soot, snow type (e.g., crystal *vs.* granular), height and structure of the vegetative canopy, and underlying surface background, among others. Unfortunately, the availability of temporal and spatial data for these discriminators is somewhat lacking.

One property that generally does not change dramatically, however, is the land surface type. While vegetative phenological conditions can change seasonally, during periods that coincide with snow coverage the vegetation is generally either at or near the full dormant (winter) state. The remnants of the vegetative canopy can protrude from and obscure the snow-covered surface, thereby dampening the reflective properties of the snow. The underlying surface reflective properties can also influence the overall radiative properties of snow-covered surfaces, especially when the snow layer is thin.

Validated data for both land surface classification (MOD12Q1, Friedl et al. 2002) and albedo (MOD43B3, 16-day product, Schaaf et al., 2002) are readily available from the Moderate Resolution Imaging Spectroradiometer (MODIS) onboard NASA's Terra (King and Herring 2000) satellite. As data for other discriminators are somewhat lacking, the goal of the present study is to aggregate the MODIS-derived snow radiative properties solely by their surface classification.

In this work, we generate snow albedo values that represent “average” snow conditions by computing ecosystem-dependant multi-year hemispherical mean and standard deviation (Jin et al. 2002). Such statistics are an amalgamation of the differing snow conditions that occur during the course of the snow season for each ecosystem type. This is accomplished by using all of the highest-quality MOD43B3 snow observations in the Northern Hemisphere over nearly five years (March 2000–December 2004).

The resulting snow albedo statistics provide researchers with reasonable and representative spectral snow albedo values that are derived from validated satellite data. They may be used as a stand-alone lookup table, or incorporated into model simulations or remote sensing retrievals by matching conditions to a lookup table of these average snow conditions. They may also be an excellent source for model validation.

This paper explores the techniques and datasets used to compute the snow albedo statistics and proceeds by providing a background on snow albedo applications and data sources (section 2), an overview of the methodology (section 3), a description of the data used and conditioning (section 4), a description of the statistical calculation (section 5), and finally a discussion of the resulting data and potential uses (section 6).

2. Background

Snow albedo is a key parameter for remote sensing of atmospheric cloud properties and plays a central role in global energy budget and climate forcing issues (Dickinson 1992; Viterbo and Betts 1999; Roesch et al. 2002; Platnick et al. 2003; King et al. 2004). Various climatic and ecosystem models, at a variety of scales, use snow-free albedo maps with superimposed snow properties (extent,

type, albedo, etc.) (Dickinson et al. 1986; 1988; Barnett et al. 1989; Versegghy 1991; Cess et al. 1991; Bonan 1996; Yang et al. 1999). Remote sensing projects depend on the knowledge of surface radiative properties for accurate observations of Earth and atmosphere properties.

Aircraft and satellite observations of snow-covered land surfaces have been undertaken for many years; various techniques have been used to derive albedo over a variety of land-cover types (see for example, McFadden and Ragotzkie 1967; Robinson and Kukla 1985; Dozier, 1989). There have also been extensive efforts to model the effects of various influencing factors (snow state, contamination, etc.) on snow albedo (Wiscombe and Warren 1980; Warren and Wiscombe 1980; Warren 1982; Dozier et al. 1981; Grenfell and Warren 1994; Davis et al. 1997; Nolin and Dozier 2000; Painter and Dozier 2004) and there are some remote sensing, ground, and laboratory validation projects that have provided observations under a variety of conditions (Salomonson and Marlatt 1968; O'Brien and Munis 1975; Brest and Goward 1987; Hall et al. 1993; Betts and Ball 1997; Klein and Stroeve 2002; Liang et al. 2002, 2005; Greuell and Oerlemans 2005; Arnold et al. 2002; Grenfell and Perovich 2004). These studies have shown that the albedo of snow-covered surfaces can vary dramatically, and therefore must be taken into account in radiative transfer calculations.

The launch of the Moderate Resolution Imaging Spectroradiometer (MODIS) onboard NASA's *Terra* spacecraft in December 1999 (King and Herring 2000) ushered in a wealth of new products with unprecedented spectral, spatial, and temporal characteristics. Of particular interest to the present study is the operational diffuse bihemispherical (white-sky) and direct beam directional hemispherical (black-sky) land surface albedo dataset, known as MOD43B3 (Schaaf et al. 2002).

This product is a validated 16-day aggregate global dataset at 1 km spatial resolution for the first seven MODIS bands, 0.47 through 2.1 μm , and for three broadbands, 0.3-0.7, 0.3-5.0, and 0.7-5.0 μm (Schaaf et al. 2002). In addition to the white-sky and black-sky spectral albedo of the Earth's land surface, this product provides a quality assurance flag that indicates if the pixel is "contaminated" by surface snow conditions. Recent validation efforts have shown that the MODIS "high quality" albedos accurately represent the general snow conditions over the pure-snow conditions of the Greenland ice sheet (Stroeve et al. 2005). In the context of the MODIS albedo product, the term "high quality" has a very specific meaning. High quality albedos refer to retrievals that had more than seven non-obscured observations over the product's 16-day period.

3. Methodology Overview

Nearly five years (March 2000- December 2004) of Northern Hemisphere MOD43B3 snow albedo observations are aggregated by the International Geosphere-Biosphere Program (IGBP) land surface classifications supplied in the MOD12Q1 land dataset. To ensure that only the highest quality albedo observations are included in the averages, the MOD43B3 Quality Assurance (QA) metrics are used to screen pixels with less than seven observations over the product's 16-day period. The MOD43B3 QA is also employed to screen pixels that are not covered with snow for more than half of the cloud-free observations over the 16-day period.

In addition, the daily $0.25^\circ \times 0.25^\circ$ horizontal resolution Near Real-Time Ice and Snow Extent (NISE) product, that is derived from satellite-borne microwave radiometers (Armstrong and Brodzik 2002), is used to further discriminate pixels

identified as snow by the MOD43B3 QA flags. Though unvalidated, this product can often provide valuable information.

4. Datasets and Conditioning

The three datasets used: MODIS albedo and land cover classification, and NISE, are stored in different projections and have different temporal periods of observation. To standardize these data for analysis, the datasets are reprojected onto a common geographical grid, a one-minute equal-angle grid, and the daily NISE data are aggregated to match the MODIS albedo 16-day period. In this section we describe the datasets used in the computations and the conditioning required to produce high quality and internally consistent statistics.

a. MODIS albedo and dataset conditioning

The MODIS 16-day global albedo product (MOD43B3/MCD43B3) is stored in a sinusoidal (SIN) projection with a series of approximately 400 tiles (one $10^\circ \times 10^\circ$ tile per file). To facilitate analysis, the raw data and QA are mosaiced onto a one-minute spatial resolution equal-angle climate modeling grid (CMG), which is ~ 2 km in spatial resolution at the equator. This procedure is a sampling process for which the geographic grid is defined and the data and QA from the nearest geolocated pixel in the MODIS tile are geospatially translocated to the CMG.

MOD43B3 pixels that were covered with snow for more than half of the cloud-free observations over the 16-day period are flagged as such in the MOD43B3 QA. Only these pixels are considered for inclusion in the statistics. To ensure that the resulting statistics provide the most accurate values possible, the pixels flagged as snow are further conditioned by applying the MODIS albedo product general and band-specific QA to remove pixels of lower quality. As detailed in the MODIS BRDF/albedo product (MOD43B) user's guide and Schaaf et

al. (2002), only pixels with seven or more observations over the 16-day period were included in the statistics; these pixels had sufficient observations to have confidence in the retrieved albedo value. Pixels flagged as water or sea ice were not considered, as this study intends to provide land-only albedo statistics.

Only the white-sky albedo (defined for diffuse surface illumination) is considered and MOD43B3 collection 4 data from March 2000 through the end of December 2004 are used. Statistics are computed for the first seven MODIS bands ranging in wavelength from 0.47 through 2.1 μm , and for three broadbands, 0.3–0.7, 0.3–5.0, and 0.7–5.0 μm .

b. MODIS ecosystem classification and dataset conditioning

The vegetative canopy and the underlying surface properties associated with land cover classification can influence the radiative effect of snow. For example, the existence of tree canopies can obscure surface snow and lower the reflectivity of the scene (e.g., McFadden and Ragotzkie 1967; Bounoua et al. 2000). To show a relationship between spectral snow albedo and land surface classification, the static MOD12Q1 ecosystem classification product, which represents the dominant land cover class for each pixel (Friedl et al. 2002), is reprojected onto a one-minute spatial resolution equal-angle CMG grid, but only for the IGBP classification scheme and associated QA arrays. At present, no QA is applied to the reprojected IGBP map, and only the predominant ecosystem classification is used for each pixel.

c. NISE snow classification and dataset conditioning

To provide further discrimination of potential snow pixels, an additional independent source of snow extent information is used. The 0.25° NISE daily snow extent product is first reprojected onto the same one-minute spatial resolution

equal-angle CMG grid. The 16-day cycle of the MOD43B3 data is matched and the number of days during this period in which NISE flags a pixel as snow is computed. Of the high quality pixels labeled as snow by MOD43B3, only the pixels that are flagged as snow by NISE for over 90% of the days during the 16-day period are included in the statistics. This logic excludes scenes in which NISE is confident ($>90\%$) that snow is present, but MOD43B3 is not flagged as snow in order to reduce the potential of non-snow MOD43B3 scenes skewing the snow albedo statistics.

5. Statistics

Many factors influence the amount of solar radiation reflected from snow-covered surfaces. Most notably, the spectral surface albedo varies as a function of snow extent, depth, type, grain size, morphology, condition (wet *vs.* dry snow), and the underlying and sometimes overlying surface type. Some of these properties can change quite dramatically over a 16-day period of MODIS albedo observations. Complicating matters, the temporal and spatial availability of these discriminators are somewhat lacking. This includes a limited number of the highest quality MOD43B3 snow albedo observations over both a 16-day period and even over the course of a full year. Additionally, MOD43B3 snow albedo observations are by nature a temporal average of changing snow conditions, except in very limited regions of continuity.

Land cover classification is one property of a pixel that does not change during a 16-day period. While vegetation phenological conditions can change seasonally, during the periods that coincide with snow coverage the vegetation is either at or near the full dormant (winter) state. The snow depth on a surface or the snow coverage in a canopy can influence the impact of the surface type on

the radiative properties. However, these snow conditions can change during the 16-day periods such that the surface effects can manifest themselves in the 16-day average albedo value.

Considering these challenges, we have analyzed the MODIS-derived spectral albedo of snow-covered surfaces as a function of IGBP ecosystem classification. The mean and standard deviation statistics provide reasonable representation of the various snow conditions that occur during the course of the year. These statistics are computed for each ecosystem class and for each of the 10 MOD43B3 narrowband and broadband wavelengths.

6. Results and discussion

The Northern Hemisphere five-year mean spectral white-sky snow albedo data are represented in Table 1 and Fig. 1. Figure 1 shows that each of the 16 IGBP ecosystem classes has a unique spectral signature, with a maximum departure of 60% at a wavelength of $0.47\ \mu\text{m}$. Surfaces that are devoid, or nearly so, of vegetation during the winter have the largest snow cover albedo (such as barren or desert, permanent snow, and cropland). The figure shows straight-line fits between discrete MODIS spectral bands for the sake of clarity only; absorption features between MODIS bands (e.g., vicinity of $1.5\ \mu\text{m}$, Grenfell and Perovich 2004) are not shown.

Ecosystems that have some vegetative canopy generally have a lower albedo. Canopied ecosystems exhibit a peak around $0.858\ \mu\text{m}$ that suggests contribution by the vegetation (leaf/needle or otherwise). Evergreen needleleaf forests have the lowest overall spectral signature, undoubtedly due to the relatively lush winter canopy that obscures the ground-level snow surface. The deciduous broadleaf and needleleaf forests have nearly identical spectral signatures, as their

winter canopies are similar. These results are in line with modeling studies that show canopies that cover snow reduce the surface albedo during winter times (Bonan 1997, Bounoua et al. 2000).

Table 2 contains the standard deviation of the white-sky albedo of snow-covered surfaces for each ecosystem classification. The majority of ecosystems exhibits standard deviations in the range 0.10-0.16 for wavelengths less than 0.86 μm , whereas the standard deviations are in the range 0.02-0.09 for wavelengths greater than 1.24 μm . This indicates variability in surface and snow conditions over the five-year period and latitudes.

The number of pixels used (not shown) to compute the statistics ranged from a high of nearly 80 million pixels for permanent snow, to a low of only 6,000 pixels for the evergreen broadleaf forest. Nine ecosystems had over a million pixels; four had over 100,000 pixels, while two had over 10,000 pixels.

These values can be incorporated into a wide variety of Earth system modeling and remote sensing or ground based research projects. One such example of integration is to use these values in tandem with the snow-free spatially complete surface albedo maps (Moody et al. 2005, 2006) to provide dynamically tailored surface albedo maps. For example, uncoupled land surface parameterization models (LSPs) can start with a base 16-day discrete wavelength snow-free spatially complete surface albedo map. Using the land cover classification and the snow extent maps they can then compute the snow albedo using statistics from the lookup table. This albedo value can either be used to drive the LSPs in resolving the surface energy balance or used as validation fields for model computed albedo. Alternatively, once snow extent and the underlying ecosystem class are defined, snow cover albedo values can be directly overlaid onto the map using Table 1.

Figure 2 provides an illustration of such a process for the $0.858\ \mu\text{m}$ data from January 1-16, 2002, in which NISE snow extent and snow type define the snow properties, and the 2000-2004 snow albedo statistics provide the albedo values. This type of procedure is currently being used operationally in the MODIS cloud optical properties product (MOD06/MYD06) (Platnick et al. 2003, King et al. 2003).

Besides the tabular format provided in Tables 1 and 2, the data are available in an Hierarchical Data Format (HDF) data file. This data file also includes the number of pixels used to provide the statistical information. The data file is available for public download via an anonymous ftp site at <ftp://modis-atmos.gsfc.nasa.gov>.

7. Conclusions

Spectral snow-covered land surface albedo is a central parameter in various Earth system studies, especially in satellite remote sensing, radiative transfer computations, and climate modeling research and simulations. Spectral snow albedo values have been shown to depend on properties such as snow extent, depth, type, grain size, morphology, condition (wet *vs* dry snow), and canopy/land surface properties. Unfortunately, the necessary temporal and spatial data needed to correlate snow albedo properly to these parameters are lacking. This includes high-quality MODIS albedo observations flagged as snow, for any particular 16-day period. In addition, any 16-day set of MOD43B3 data is by its very nature a temporal average of changing snow conditions.

Land cover type and phenology do not change substantially during any winter 16-day period. As such, the spectral albedo of “average” snow conditions, according to IGBP ecosystem classification, is provided. These values are com-

puted over a five-year period (2000-2004) using high quality MOD43B3 data flagged as snow. As an additional and independent layer of information, NISE data were used to check that these candidate pixels were indeed snow covered over the majority of each 16-day period.

In this paper, we present a five-year mean and standard deviation of Northern Hemisphere spectral snow albedo for the 16 IGBP ecosystem classes and for each of the 10 MOD43B3 narrowband and broadband wavelengths. Each ecosystem classification has a unique spectral snow albedo signature since both the winter canopy and underlying surface radiative properties impact the reflectivity of the snow overlying these surfaces.

These albedo values can be used in stand-alone lookup tables or incorporated into model simulations or remote sensing retrievals of clouds from satellite (Platnick et al. 2003) or aerosols from ground-based Aerosol Robotic NETwork (AERONET) sunphotometer observations (Holben et al. 1998; Dubovik et al. 2000). They provide representative spectral snow albedo values derived from validated satellite observations.

Acknowledgments

The research reported in this article was supported by EOS MODIS support, the MODIS Science Team under NASA contract 621-30-H4, and to Goddard Space Flight Center (EGM, MDK, DKH, SP) and NASA contract NAS5-31369 to Boston University (CBS). The authors would like to express their appreciation to Dr. Lahouari Bounoua, Goddard Space Flight Center, for providing valuable insight into modeling community requirements and reviewing the methodologies used in this work.

REFERENCES

- Armstrong, R. L., and M. J. Brodzik, 2002: Hemispheric-scale comparison and evaluation of passive-microwave snow algorithms. *Ann. Glaciol.*, **34**, 38–44.
- Arnold, G. T., S. C. Tsay, M. D. King, J. Y. Li, and P. F. Soulen, 2002: Airborne spectral measurements of surface-atmosphere anisotropy for Arctic sea ice and tundra. *Int. J. Remote Sens.*, **23**, 3763–3781.
- Barnett, T. P., L. Dumenil, U. Schlese, E. Roeckner, and M. Latif, 1989: The effect of Eurasian snow cover on regional and global climate variations. *J. Atmos. Sci.*, **46**, 661–685.
- Betts, A. K., and J. H. Ball, 1997: Albedo over the boreal forest. *J. Geophys. Res.*, **102**, 28901–28909.
- Bonan, G. B., 1996: A land surface model (LSM version 1.0) for ecological, hydrological, and atmospheric studies: Technical description and user's guide. NCAR Tech. Note NCAR/TN2417+STR, 150 pp. [Available from NCAR, P. O. Box 3000, Boulder, CO 80307-3000.]
- _____, 1997: Effects of land use on the climate of the United States. *Climatic Change*, **37**, 449–486.
- Bounoua, L., G. J. Collatz, S. O. Los, P. J. Sellers, D. A. Dazlich, C. J. Tucker and D. Randall, 2000: Effects of land cover conversion on surface climate. *J. Climate*, **13**, 2277–2292.
- Brest, C. L., and S. N. Goward, 1987: Deriving surface albedo measurements from narrow band satellite data. *Int. J. Remote Sens.*, **8**, 351–367.
- Cess, R. D., and Coauthors, 1991: Intercomparison of snow-feedback as produced by general circulation models. *Science*, **253**, 888–892.
- Davis, R. E., J. P. Hardy, W. Ni, C. Woodcock, C. J. McKenzie, R. Jordan, and X. Li, 1997: Variation of snow ablation in the boreal forest: A sensitivity study

- on the effects of conifer canopy. *J. Geophys. Res.*, **102**(D24), 29389–29396.
- Dickenson, R. E., 1988: The force-restore model for surface temperature and its generalizations. *J. Climate*, **1**, 1086–1097.
- _____, A. Henderson-Sellers, P. J. Kennedy, and M. F. Wilson, 1986: Community Climate Model. NCAR Tech. Note NCAR/TN2275+STR, 69 pp. [Available from NCAR, P.O. Box 3000, Boulder, CO 80307-3000.]
- _____, 1992: Land Surface. In *Climate System Modeling*, edited by K. E. Trenberth, Cambridge University Press, pp. 149–171.
- Dozier, J., 1989: Spectral signature of alpine snow cover from the Landsat Thematic Mapper. *Remote Sens. Environ.*, **28**, 9–22.
- _____, S. R. Schneider and D. F. McGuinness, 1981: Effect of grain size and snow-pack water equivalence on visible and near-infrared satellite observations of snow. *Water Resources Res.*, **17**, 1213–1221.
- Dubovik, O., A. Smirnov, B. N. Holben, M. D. King, Y. J. Kaufman, T. F. Eck, and I. Slutsker, 2000: Accuracy assessments of aerosol optical properties retrieved from AERONET sun and sky-radiance measurements. *J. Geophys. Res.*, **105**, 9791–9806.
- Friedl, M. A., D. K. McIver, J. C. F. Hodges, X. Y. Zhang, D. Muchoney, A. H. Strahler, C. E. Woodcock, S. Gopal, A. Schneider, A. Cooper, A. Baccini, F. Gao, and C. Schaaf, 2002: Global land cover mapping from MODIS: Algorithms and early results. *Remote Sens. Environ.*, **83**, 287–302.
- Grenfell, T. C., and S. G. Warren, 1994: Reflection of solar radiation by the Antarctic snow surface at ultraviolet, visible and near-infrared wavelengths. *J. Geophys. Res.*, **99**, 18669–18684.
- _____, and D. K. Perovich, 2004: Seasonal and spatial evolution of albedo in a snow-ice-land-ocean environment. *J. Geophys. Res.*, **109**, C01001,

doi:10.1029/2003JC001866.

- Greuell, W., and J. Oerlemans, 2005: Validation of AVHRR- and MODIS-derived albedos of snow and ice surfaces by means of helicopter measurements. *J. Glaciology*, **51**, 37–48.
- Hall, D. K., J. L. Foster, J. R. Irons, and P. W. Dabney, 1993: Airborne bidirectional radiances of snow-covered surfaces in Montana, U.S.A. *Ann. Glaciology*, **17**, 35–40.
- Holben, B. N., T. F. Eck, I. Slutsker, D. Tanré, J. P. Buis, A. Setzer, E. Vermote, J. A. Reagan, Y. J. Kaufman, T. Nakajima, F. Lavenu, I. Jankowiak, and A. Smirnov, 1998: AERONET—A federated instrument network and data archive for aerosol characterization. *Remote Sens. Environ.*, **66**, 1–16.
- Jin, Y., C. Schaaf, F. Gao, X. Li, A. Strahler, X. Zeng, R. Dickinson, 2002: How does snow impact the albedo of vegetated land surfaces as analyzed with MODIS data? *Geophys. Res. Lett.*, **29**, doi:10.1029/2001GL014132.
- King, M. D., and D. D. Herring, 2000: Monitoring Earth's vital signs. *Sci. Amer.*, **282**, 72–77.
- _____, W. P. Menzel, Y. J. Kaufman, D. Tanré, B. C. Gao, S. Platnick, S. A. Ackerman, L. A. Remer, R. Pincus, and P. A. Hubanks, 2003: Cloud and aerosol properties, precipitable water, and profiles of temperature and humidity from MODIS. *IEEE Trans. Geosci. Remote Sens.*, **41**, 442–458.
- _____, S. Platnick, P. Yang, G. T. Arnold, M. A. Gray, J. C. Riédi, S. A. Ackerman, and K. N. Liou, 2004: Remote sensing of liquid water and ice cloud optical thickness and effective radius in the arctic: Application of airborne multispectral MAS data. *J. Atmos. Oceanic Technol.*, **21**, 857–875.
- Klein, A. G., and J. Stroeve, 2002: Development and validation of a snow albedo algorithm for the MODIS instrument. *Ann. Glaciology*, **34**, 45–52.

- Liang S., H. Fang, M. Chen, C. J. Shuey, C. Walthall, C. Daughtry, J. Morisette, C. Schaaf, and A. Strahler, 2002: Validating MODIS land surface reflectance and albedo products: Methods and preliminary results. *Remote Sens. Environ.*, **83**, 149–162.
- _____, J. Stroeve, and J. E. Box, 2005: Mapping daily snow/ice shortwave broadband albedo from Moderate Resolution Imaging Spectroradiometer (MODIS): The improved direct retrieval algorithm and validation with Greenland in situ measurement. *J. Geophys. Res.*, **110**, D10109, doi:10.1029/2004JD005493.
- McFadden, J. D., and R. A. Ragotzkie, 1967: Climatological significance of albedo in central Canada. *J. Geophys. Res.*, **72**, 1135–1143.
- Moody, E. G., M. D. King, S., Platnick, C. B. Schaaf, and F. Gao, 2005: Spatially complete global spectral surface albedos: Value-added datasets derived from Terra MODIS land products. *IEEE Trans. Geosci. Remote Sens.*, **43**, 144–158.
- _____, _____, _____, and _____, 2006: Comparison of temporal trends in the spatially complete global spectral surface albedo products. Submitted to *IEEE Trans. Geosci. Remote Sens.*
- Nolin, A. W., and J. Dozier, 2000: A hyperspectral method for remotely sensing the grain size of snow. *Remote Sens. Environ.*, **74**, 207–216.
- O'Brien, H. W., and R. H. Munis, 1975: Red and near-infrared spectral reflectance of snow. Cold Regions Research and Engineering Laboratory Research Report 332, 18 pp.
- Platnick, S., M. D. King, S. A. Ackerman, W. P. Menzel, B. A. Baum, J. C. Riédi, and R. A. Frey, 2003: The MODIS cloud products: Algorithms and examples from Terra. *IEEE Trans. Geosci. Remote Sens.*, **41**, 459–473.

- Robinson, D. A., and G. Kukla, 1985: Maximum surface albedo of seasonally snow-covered lands in the Northern Hemisphere. *J. Climate and Appl. Meteor.*, **24**, 402–411.
- Roesch, A., M. Wild, R. Pinker, and A. Ohmura, 2002: Comparison of spectral surface albedos and their impact on the general circulation model simulated surface climate. *J. Geophys. Res.*, **107**, 4221, doi:10.1029/2001JD000809.
- Salomonson, V. V., and W. E. Marlatt, 1968: Anisotropic solar reflectance over white sand, snow and stratus clouds. *J. Appl. Meteor.*, **7**, 475–483.
- Stroeve, J., J. Box, F. Gao, S. Liang, A. Nolin, and C. Schaaf, 2005: Accuracy assessment of the MODIS 16-day albedo product for snow: Comparisons with Greenland in situ measurements. *Remote Sens. Environ.*, **94**, 46–60.
- Schaaf, C. B., F. Gao, A. H. Strahler, W. Lucht, X. W. Li, T. Tsang, N. C. Strugnell, X. Y. Zhang, Y. F. Jin, J. P. Muller, P. Lewis, M. Barnsley, P. Hobson, M. Disney, G. Roberts, M. Dunderdale, C. Doll, R. P. d'Entremont, B. X. Hu, S. L. Liang, J. L. Privette, and D. Roy, 2002: First operational BRDF, albedo nadir reflectance products from MODIS. *Remote Sens. Environ.*, **83**, 135–148.
- Verseghy, D. L., 1991: CLASS—A Canadian land surface scheme for GCMs. Part I: Soil model. *Int. J. Climatol.*, **11**, 111–133.
- Viterbo, P., and A. K. Betts, 1999: Impact on ECMWF forecasts of changes to the albedo of the boreal forests in the presence of snow. *J. Geophys. Res.*, **104**, 27803–27810.
- Warren, S. G., 1982: Optical properties of snow. *Rev. Geophys. Space Phys.*, **20**, 67–89.
- _____, and W. J. Wiscombe, 1980: A model for the spectral albedo of snow. II: Snow containing atmospheric aerosols. *J. Atmos. Sci.*, **37**, 2734–2745.
- Wiscombe, W. J., and S. G. Warren, 1980: A model for the spectral albedo of

snow. I: Pure snow. *J. Atmos. Sci.*, **37**, 2712–2733.

Yang, Z. L., R. E. Dickinson, A. N. Hahmann, G. Y. Niu, M. Shaikh, X. Gao, R. C. Bales, S. Sorooshian, and J. M. Jin, 1999: Simulation of snow mass and extent in global climate models. *Hydrological Processes*, **13** (12-13), 2097–2113.

TABLE CAPTIONS

- Table 1. Northern Hemisphere five-year (2000-2004) spectral white-sky snow albedo mean values by IGBP ecosystem classification and band.
- Table 2. Northern Hemisphere five-year (2000-2004) spectral white-sky snow albedo standard deviation values by IGBP ecosystem classification and band.

TABLE 1. Northern Hemisphere five-year (2000-2004) spectral white-sky snow albedo mean values by IGBP ecosystem classification and band.

Ecosystem	White-sky snow albedo by wavelength (μm)									
	0.47	0.55	0.69	0.86	1.24	1.64	2.13	0.3- 0.7	0.7- 5.0	0.3- 5.0
Evergreen										
Needle Forest	0.356	0.355	0.331	0.396	0.236	0.090	0.046	0.309	0.242	0.273
Evergreen Broad										
Forest	0.490	0.488	0.470	0.501	0.306	0.114	0.062	0.442	0.328	0.384
Deciduous										
Needle Forest	0.425	0.421	0.410	0.421	0.259	0.118	0.071	0.390	0.268	0.327
Deciduous Broad										
Forest	0.428	0.430	0.412	0.459	0.264	0.104	0.056	0.346	0.272	0.308
Mixed Forest	0.388	0.391	0.370	0.431	0.251	0.098	0.052	0.318	0.254	0.285
Closed Shrubs	0.482	0.477	0.456	0.472	0.286	0.112	0.063	0.421	0.298	0.359
Open Shrubs	0.727	0.717	0.699	0.673	0.372	0.120	0.058	0.677	0.443	0.560
Woody Savanna	0.471	0.463	0.443	0.470	0.276	0.106	0.056	0.436	0.299	0.365
Savanna	0.586	0.593	0.584	0.589	0.309	0.105	0.053	0.566	0.386	0.473
Grassland	0.723	0.724	0.714	0.696	0.386	0.117	0.057	0.695	0.476	0.586
Wetland	0.687	0.696	0.689	0.672	0.322	0.095	0.043	0.664	0.439	0.549
Cropland	0.759	0.761	0.755	0.737	0.396	0.112	0.051	0.688	0.469	0.579
Urban	0.537	0.539	0.526	0.546	0.303	0.106	0.056	0.499	0.339	0.417
Crop Mosaic	0.652	0.656	0.644	0.648	0.358	0.113	0.056	0.591	0.414	0.502
Permanent Snow	0.950	0.944	0.917	0.838	0.445	0.118	0.053	0.889	0.572	0.735
Barren/Desert	0.872	0.868	0.849	0.798	0.423	0.124	0.059	0.779	0.514	0.648

Table 2. Northern Hemisphere five-year (2000-2004) spectral white-sky snow albedo standard deviation values by IGBP ecosystem classification and band.

Ecosystem	Standard deviation of white-sky snow albedo by wavelength (μm)									
	0.47	0.55	0.69	0.86	1.24	1.64	2.13	0.3- 0.7	0.7- 5.0	0.3- 5.0
Evergreen										
Needle Forest	0.114	0.116	0.122	0.106	0.062	0.021	0.011	0.137	0.084	0.104
Evergreen Broad										
Forest	0.144	0.147	0.157	0.143	0.080	0.026	0.018	0.169	0.109	0.135
Deciduous										
Needle Forest	0.076	0.078	0.081	0.079	0.056	0.022	0.014	0.103	0.072	0.083
Deciduous Broad										
Forest	0.111	0.111	0.115	0.101	0.067	0.024	0.015	0.117	0.076	0.092
Mixed Forest	0.137	0.139	0.147	0.121	0.070	0.024	0.014	0.140	0.087	0.108
Closed Shrubs	0.121	0.122	0.131	0.122	0.070	0.026	0.017	0.154	0.102	0.125
Open Shrubs	0.152	0.155	0.159	0.141	0.094	0.031	0.016	0.170	0.130	0.149
Woody Savanna	0.115	0.117	0.125	0.107	0.072	0.028	0.017	0.141	0.096	0.114
Savanna	0.115	0.118	0.123	0.114	0.088	0.031	0.017	0.142	0.104	0.118
Grassland	0.153	0.155	0.161	0.148	0.091	0.028	0.017	0.162	0.124	0.142
Wetland	0.120	0.118	0.119	0.113	0.105	0.037	0.016	0.138	0.107	0.120
Cropland	0.116	0.114	0.116	0.101	0.083	0.028	0.015	0.146	0.106	0.125
Urban	0.130	0.131	0.137	0.124	0.086	0.028	0.015	0.147	0.101	0.121
Crop Mosaic	0.166	0.167	0.173	0.144	0.089	0.025	0.014	0.175	0.119	0.147
Permanent Snow	0.067	0.064	0.069	0.087	0.103	0.040	0.019	0.114	0.106	0.112
Barren/Desert	0.099	0.101	0.107	0.108	0.091	0.031	0.017	0.158	0.127	0.143

FIGURE LEGENDS

- Fig. 1. Northern Hemisphere five-year average white-sky spectral snow albedo as a function of IGBP ecosystem classification. The statistics are derived from 2000-2004 MOD43B3 collection 4, MOD12Q1, and NISE data. Sea ice is excluded from this analysis.
- Fig. 2. 0.858 μm white-sky snow-free spatially complete albedo data from January 1-16, 2002, without (top) and with (bottom) overlaid snow albedo values. Pixels flagged as snow by the NISE snow extent product have their snow-free values replaced with ecosystem-dependant snow albedo values. The snow albedo values are provided from the lookup table provided from the 2000-2004 Northern Hemisphere spectral snow albedo statistics.

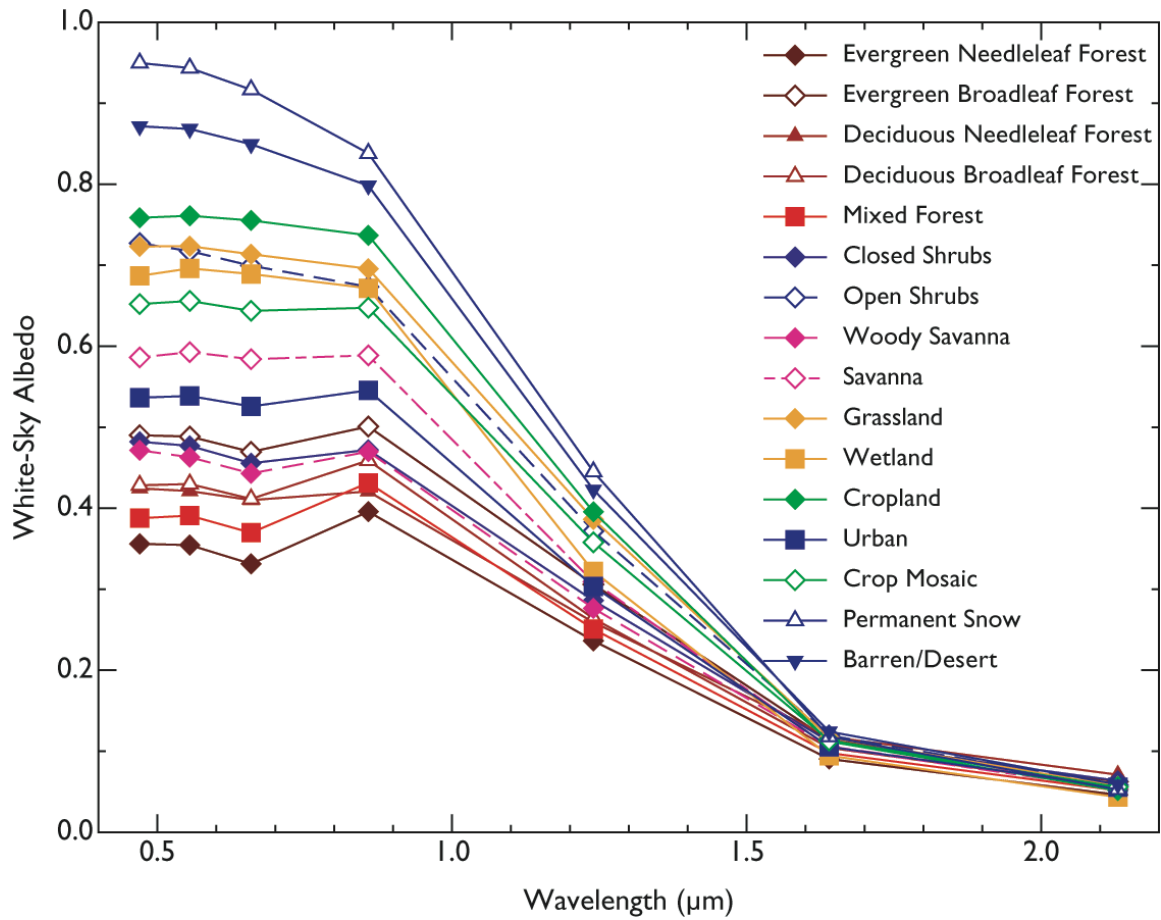


Fig. 1. Northern Hemisphere five-year average white-sky spectral snow albedo as a function of IGBP ecosystem classification. The statistics are derived from 2000-2004 MOD43B3 collection 4, MOD12Q1, and NISE data. Sea ice is excluded from this analysis.

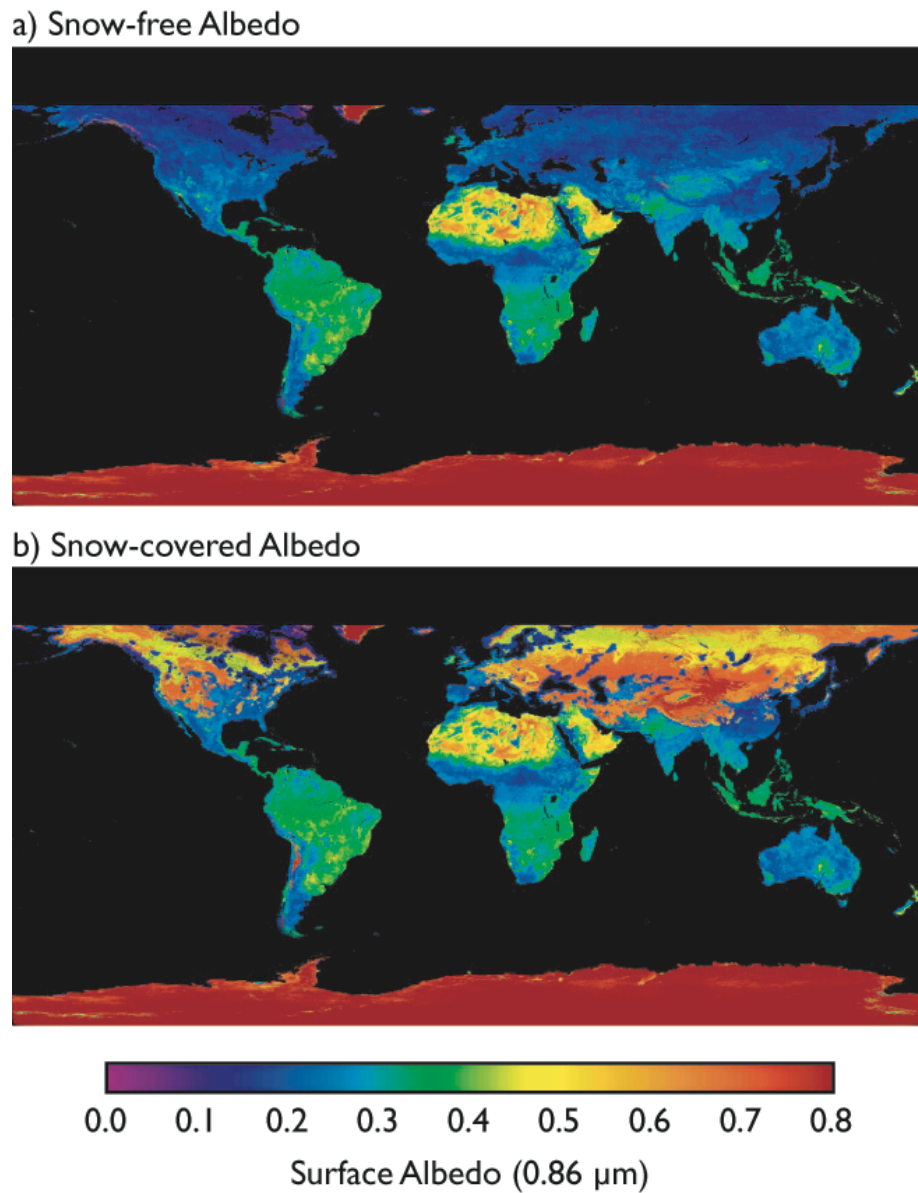


Fig. 2. $0.858 \mu\text{m}$ white-sky snow-free spatially complete albedo data from January 1-16, 2002, without (top) and with (bottom) overlaid snow albedo values. Pixels flagged as snow by the NISE snow extent product have their snow-free values replaced with ecosystem-dependant snow albedo values. The snow albedo values are provided from the lookup table provided from the 2000-2004 Northern Hemisphere spectral snow albedo statistics.